Mon. Not. R. Astron. Soc. **391,** 1913–1924 (2008) doi:10.1111/j.1365-2966.2008.14014.x

Photometric variability of the T Tauri star TW Hya on time-scales of hours to years⋆

Slavek M. Rucinski,[1†] Jaymie M. Matthews,[2] Rainer Kuschnig,[2] Grzegorz Pojmański,[3] Jason Rowe,[4] David B. Guenther,[5] Anthony F. J. Moffat,[6,7] Dimitar Sasselov,[8] Gordon A. H. Walker[2] and Werner W. Weiss[9]

[1]*Department of Astronomy and Astrophysics, University of Toronto, 50 St George St, Toronto, Ontario, M5S 3H4, Canada*
[2]*Department of Physics & Astronomy, University of British Columbia, 6224 Agricultural Road, Vancouver, B.C., V6T 1Z1, Canada*
[3]*Warsaw University Astronomical Observatory, Al. Ujazdowskie 4, 00–478 Warszawa, Poland*
[4]*NASA-Ames Research Park, MS-244-30 Building 244, Rm 107A Moffett Field, CA 94035-1000, USA*
[5]*Institute for Computational Astrophysics, Department of Astronomy and Physics, Saint Marys University, Halifax, N.S., B3H 3C3, Canada*
[6]*Département de Physique, Université de Montréal, C.P.6128, Succursale: Centre-Ville, Montréal, QC, H3C 3J7, Canada*
[7]*Centre de Researche en Astrophysique du Québec, Canada*
[8]*Harvard-Smithsonian Center for Astrophysics, 60 Garden Street, Cambridge, MA 02138, USA*
[9]*Institut für Astronomie, Universität Wien, Türkenschanzstrasse 17, A-1180 Wien, Austria*

Accepted 2008 September 25. Received 2008 September 25; in original form 2008 September 3

ABSTRACT

Microvariability & Oscillations of STars (MOST) and All Sky Automated Survey (ASAS) observations have been used to characterize photometric variability of TW Hya on time-scales from a fraction of a day to 7.5 weeks and from a few days to 8 yr, respectively. The two data sets have very different uncertainties and temporal coverage properties and cannot be directly combined, nevertheless, they suggest a global variability spectrum with 'flicker-noise' properties, that is with amplitudes $a \propto 1/\sqrt{f}$, over >4 decades in frequency, in the range $f = 0.0003$–$10\,\mathrm{c\,d^{-1}}$. A 3.7 d period is clearly present in the continuous 11 d, 0.07 d time resolution, observations by MOST in 2007. Brightness extrema coincide with zero-velocity crossings in periodic (3.56 d) radial-velocity variability detected in contemporaneous spectroscopic observations of Setiawan et al. and interpreted as caused by a planet. The 3.56/3.7 d periodicity was entirely absent in the second, 4 times longer MOST run in 2008, casting doubt on the planetary explanation. Instead, a spectrum of unstable single periods within the range of 2–9 d was observed; the tendency of the periods to progressively shorten was well traced using the wavelet analysis. The evolving periodicities and the overall flicker-noise characteristics of the TW Hya variability suggest a combination of several mechanisms, with the dominant ones probably related to the accretion processes from the disc around the star.

Key words: stars: pre-main-sequence – stars: variables: other.

1 INTRODUCTION

Photometric variability of the very young T Tauri-type stars is still puzzling and remains an object of very active research; for the most recent literature, see Percy, Gryc & Wong (2006) and Grankin et al. (2007). The variability comes in part from accretion and matter ejection phenomena, in part from photospheric spots coming and going into view and in part from the inner accretion disc, and then the accretion region as matter is channelled by magnetic fields into the photosphere. Herbst, Herbst & Grossman (1994) identified three basic types of variability which may co-exist in a given T Tauri star: Type I, photospheric dark spots; Type II, variable accretion with some rotation modulation component; Type III, totally random variations, mostly due to variable obscuration. Quasi-periodic variations intertwined with chaotic changes are the most natural outcome of several different mechanisms contributing simultaneously.

Typical time-scales of T Tauri stars are of the order of hours to days, but they are very difficult to characterize from the ground

⋆Based on data from the MOST satellite, a Canadian Space Agency mission jointly operated by Dynacon Inc., the University of Toronto Institute for Aerospace Studies and the University of British Columbia, with the assistance of the University of Vienna, and on data from the All Sky Automated Survey (ASAS) conducted by the Warsaw University Observatory, Warsaw, Poland at the Las Campanas Observatory, Chile.

†E-mail: rucinski@astro.utoronto.ca

because of diurnal observation breaks and discontinuous temporal coverage. We are not aware of any attempt to obtain a continuous record of T Tauri variability from a satellite or through inter-observatory coordination of efforts.

In this paper, we present new, single broad-band (located between *V* and *R* bands), continuous photometric observations of the T Tauri star TW Hya obtained by the Microvariability & Oscillations of STars (MOST) satellite mission over 11 d in 2007 and 46 d in 2008. Although the high-frequency coverage (above $10\,\mathrm{c\,d^{-1}}$) was inadequate, the temporal coverage at the once-per-orbit satellite sampling period of 101.4 min was practically uninterrupted permitting a study of the stellar variability on time-scales of a fraction of a day to a few tens of days. For still longer time-scales, we used the All Sky Automated Survey (ASAS) project data obtained over 8-yr seasons from 2001 to 2008. These data sampled the brightness changes of TW Hya in the *V* and *I* bands at intervals of a day to a few days.

In this paper, after a brief introduction of TW Hya itself (Section 2) and of its previous photometric variability studies (Section 3), we discuss the results of the analysis of the 2007 and 2008 MOST data (Sections 4 and 5). The TW Hya variability at very low frequencies is analysed on the basis of the ASAS data (Section 6). We conclude (Sections 7 and 8) that TW Hya shows a flicker-noise variability spectrum (the special type of a 'red noise' spectrum) over a wide range of the time-scale from hours to years.

2 THE TARGET, TW HYA

Following the suggestion of Herbig (1978), Rucinski & Krautter (1983) established that TW Hya (J2000: 11:01:51.9, −34:42:17) is a genuine, if isolated T Tauri star. Its spectral type is K7V and the spectrum is typical for the class with strong hydrogen line emission, with the Li 6707 Å line present. It shows a complex and apparently irregular photometric variability. The spatial isolation of TW Hya was puzzling and hard to explain. It appears on an empty sky field, far from any regions of star formation or other groupings of T Tauri stars. Later, however, an intense effort started by de la Reza et al. (1989) and continuing through several subsequent studies [e.g. Webb et al. (1999); Zuckerman et al. (2001)] has led to a realization that TW Hya is part of a loose and dispersed association of young, nearby stars. But, it is the only one of two stars [the other is TWA 3A = Hen 3–600A; Jayawardhana et al. (2006)] among them which continue to show disc accretion; the remaining stars, members of what is now called the TW Hya Association (TWA), have properties of post-T Tauri stars, i.e. still show a high abundance of lithium, rapid rotation and resulting spot activity, but no direct signs of disc accretion. While the TWA has about 25 definite members, Song, Zuckerman & Bessell (2003) broadened the definition of the association and added more young members from other groups so that the current count is about 45 stars.

In this paper, we limit ourselves to a study of the photometric variability of TW Hya, treating it as a typical T Tauri star. In fact, it is the nearest star of this type. Analysis of raw *Hipparcos* data (Wichmann et al. 1998) determined a moderately accurate parallax of 17.72 ± 2.21 mas, corresponding to a distance of 56 ± 7 pc, putting TW Hya some twice as close as any other T Tauri star. New reductions of the *Hipparcos* data (van Leeuwen 2007) gave a parallax of 18.04 ± 3.08 mas (55 ± 9 pc) confirming the previous determination.

Rucinski & Krautter (1983) observed variability of TW Hya within $10.9 < V < 11.25, 0.8 < B - V < 1.2$ and $1.5 < V - I < 1.8$ and noted strong linear correlations between these quantities (see fig. 2 in that paper). However, the *mean values* of the two colour indices are not consistent: for the observed $V - I = 1.55$, an effective temperature of about 4000 K would imply $B - V \simeq 1.3$, whereas $B - V \simeq 0.90$ is observed.

Of interest to the interpretation of the variability of TW Hya is the low inclination of its rotational axis and of its accretion disc. TW Hya appears to be visible nearly pole-on at a very low inclination angle, most likely $i < 15^\circ$ (Krist et al. 2000; Qi et al. 2004). Setiawan et al. (2008) quote values of $i = 7^\circ \pm 1^\circ$ and $14^\circ \pm 4^\circ$. Torres et al. (2003) found $V \sin i = 4\,\mathrm{km\,s^{-1}}$ and cited several previous estimates of $V \sin i$: 4, 5, 10, 13, 14 and 15 km s^{-1}. Jayawardhana et al. (2006) gave the new estimate of $V \sin i = 10.6\,\mathrm{km\,s^{-1}}$. Because the rotation period is likely to be of the order of 2–4 d, the low $V \sin i$ values imply a small inclination angle. The exact value is unimportant here; the crucial point is that the inner accretion disc is completely visible, in contrast to many other T Tauri stars which are – in the majority – detected with the normal probability of the inclination angle which scales as $\sin i$, i.e. usually they have large axial inclinations and are seen more edge-on.

3 PREVIOUS OBSERVATIONS OF THE PHOTOMETRIC VARIABILITY OF TW HYA

TW Hya shows a rich but confusing photometric variability. Rucinski & Krautter (1983) saw large night-to-night variations of $\pm$ 0.2 mag in *V*. From a few repeated nightly observations, they suggested rapid variability on time-scales as short as 0.21 d. Later, Rucinski (1988) saw indications of a 2 d time-scale regularity. Several temporal variability investigations followed as summarized in Lawson & Crause (2005). They indicated characteristic variability periods of 2.88 d from *Hipparcos* photometric data (Koen & Eyer 2002), 2.85 d from Hβ linewidth variations and 4.4 d from *B* band veiling changes (Alencar & Batalha 2002). Lawson & Crause (2005) finally chose the period of 2.8 d as the main, characteristic periodicity, but only after an arbitrary removal of about one-fourth of their data covering about 40 per cent of the whole duration of their observing run.

Herbst et al. (1994) suggested that TW Hya belongs to the Type IIp of the T Tauri variables with the accretion variability combined with a semiperiodic rotation modulation component. The Type IIp variables are characterized by periodic variations that persist for some time.

Recently, precise radial velocities of TW Hya obtained by Setiawan et al. (2008) revealed a clear spectroscopic sinusoidal signal with a period of 3.56 d and amplitude of $\pm$ 200 m s^{-1}. The authors interpreted it as an indication of a massive planet situated inside the accretion disc, close to the surface of the star, with orbital semimajor axis of only 0.041 au = $8.8\,\mathrm{R_\odot}$. To be sure that this is really the signal of planet revolution rather than that of the line-centroid spot modulation reflecting star rotation, they re-analysed (as summarized in the Supplementary material to this paper) all previous photometric data for TW Hya. This gave several acceptable periods in the ranges of 1.74–1.98, 1.98–2.38 and 1.80–2.20 d, which were finally merged into an estimate of 2.1 ± 0.5 d. This period was identified as the period of rotation of TW Hya, as distinct from the 3.56 d radial-velocity modulation. Several other periodicities were excluded in this process, but another one surfaced with a period of 9.05 d, as seen in the changes of the Hα equivalent width. We note that the planetary explanation of the radial-velocity changes has been recently questioned by Huélamo et al. (2008) who propose photospheric spot-induced spectral line shifts instead.

Clearly, the picture of TW Hya temporal variability is a very complex one. All previously suggested periods, 2.0, 2.1, 2.8, 2.85, 2.85, 4.4 and 9.05 d – in addition to the three ranges suggested by Setiawan et al. (2008) – require confirmation, particularly in view of the new radial-velocity discovery of the strong (but still different) spectroscopic periodicity of 3.56 d. We have been fortunate that – through sheer coincidence – the MOST satellite observed TW Hya photometrically exactly during the time when radial-velocity observations of Setiawan et al. (2008) were collected. The satellite run lasted 11 d and indeed led to detection of a well-defined photometric period of 3.7 d; for such a short run, this value is in fact consistent with 3.56 d. Because of the significance of this result and the 2007 MOST run was too short to define this period well, we re-observed TW Hya in 2008 over a time-span of 4 times longer than in 2007. The unexpected and intriguing results of both MOST runs form the main part of this paper.

4 MOST 2007 OBSERVATIONS

4.1 The data

MOST is a microsatellite housing a 15-cm telescope which feeds a CCD photometer through a single custom, broad-band, optical filter (350–700 nm). The effective wavelength of the single, broad-band filter is located between the *V* and *R* bands. The pre-launch characteristics of the mission are described by Walker et al. (2003) and the initial post-launch performance by Matthews et al. (2004). MOST is in a Sun-synchronous polar orbit (820 km altitude) from which it can monitor some stars for as long as two months without interruption, provided they are located in the ecliptic part of the sky with declinations roughly in the range of -18° to $+35^\circ$. The instrument was designed to obtain highly precise photometry of bright stars through Fabry-lens imaging, but direct imaging of fainter objects permits photometry in the magnitude range of about 6–11 mag with typical accuracy of a few 0.001 mag. Since the loss of the attitude control CCD system in 2006 and the need to use the science CCD for the satellite stabilization, the data are obtained by stacking several short, 1–2 s exposures into typically 30 s data points. With the mean $\bar{V} \simeq 11.0$ and $\bar{I} \simeq 9.3$ (see Section 6), TW Hya is close to the faint limit of the MOST capabilities.

In 2007, MOST observed TW Hya for 11.4 d between 2007 March 14 and March 25. With declination $-34^\circ 42'$, TW Hya is located outside the continuous visibility zone of the satellite. For that reason, the satellite had to be repeatedly re-oriented to a 'parking' object for part of its orbit (31 Comae in 2007). This slightly affected the accuracy of the data, increased the instrumental noise which is due to stray light and South Atlantic Anomaly passages and spoiled the shape of the Fourier spectral window. In the analysis, for the sake of the uniformity of the data, we sacrificed all variability information within each satellite orbit and formed single points separated on the average by 101 min.

For the 2007 observations, the median value of the mean photometric error per one satellite-orbit point, resulting from averaging of 30–80 individual, 1/2-min exposures spanning 15–40 min of time, was 0.0026 of the mean flux level. This number includes variability of the star within each satellite orbit. The observed range of the mean errors was 0.001–0.005, with a few observations with errors reaching 0.0075.

Variability of the star was certainly visible within each satellite orbit, but (1) it was of a small amplitude, which is attested by small values of mean standard errors formed from the individual satellite orbits (see the third column of Table 1) and agrees with our main conclusions on the dominant 'flicker-noise' variability (see further in this paper) and (2) aliasing due to the variable duration of the orbital scans was severe. Thus, we analysed only periods corresponding to frequencies of $13\,\mathrm{c\,d^{-1}}$ or less; however, for simplicity, we have limited the analysis to frequencies $f < 10\,\mathrm{c\,d^{-1}}$.

Table 1. TW Hya: MOST 2007 and 2008 observations; single data points per each satellite orbit. The whole table is available on-line only.

(1) t	(2) Mean flux	(3) Error	(4) n
4174.0148	1.1560	0.0026	32
4174.0786	1.4284	0.0023	75
4174.1481	1.3983	0.0034	77
4174.2180	1.4437	0.0042	76
4174.2845	1.3854	0.0037	52

The columns: (1) $t = JD - 2\,450\,000$; (2) the photometric flux of TW Hya for each satellite orbit, independently normalized to the mean value for the 2007 and 2008 observing runs; (3) the mean standard error of the normalized flux estimated from the scatter of 30–80 individual 0.5 min integrations; (4) the number of individual observations contributing to the mean and used to evaluate the errors.

The 2007 data are shown in Fig. 1 and are tabulated in Table 1; this table contains also the MOST 2008 data discussed below. The heliocentric time used in this paper is $t = JD - 2\,450\,000$. The following features should be noted in Fig. 1: (i) the light curve consists of a gentle, but very well-defined undulation with superimposed brightening events lasting typically a fraction of a day, (ii) the slow variability shows three minima and four maxima indicating an underlying period of about 3.5 d and (iii) the overall variation appears to show larger amplitudes for longer time-scales, a property may be characteristic for some type of 'red noise'.

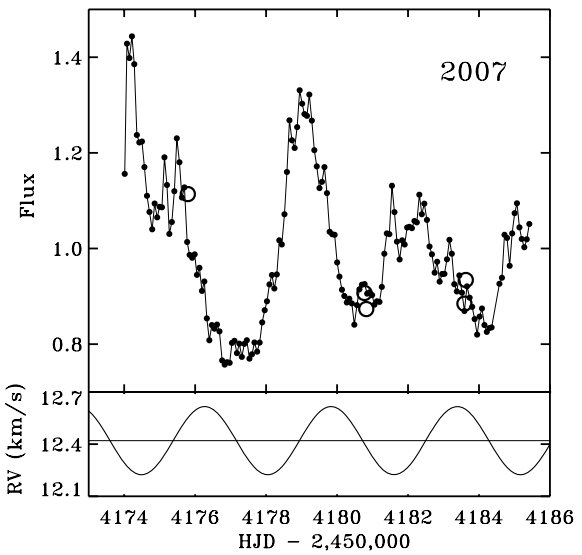

Figure 1. The MOST data normalized to the average flux from 11.4 d of observations of TW Hya in 2007. The filled, connected and small circles give the mean flux values for each satellite orbit (the spacing is 0.0705 d; in two cases, twice as long). The large circles show the ASAS *V*-band observations, transformed to intensities, with the assumed mean value of $\bar{V} = 11.04$ (Section 6). The lower panel gives the schematic radial-velocity variations, based on the observations of Setiawan et al. (2008) obtained just days before and after the 2007 MOST observations.

4.2 Fourier analysis of the 2007 time series

The Fourier analysis of the 2007 data was done by simple least-squares fits of expressions of the form $l(f) = c_0(f) + c_1(f)\cos[2\pi(t - t_0)f] + c_2(f)\sin[2\pi(t - t_0)f]$ for a range of frequencies $0.01 \leq f \leq 10$ c d^{-1}. For the 2007 data, the frequency step was $\Delta f = 0.01$. The bootstrap sampling technique permitted evaluation of mean standard errors of the amplitudes from the spread of the coefficients a_i. This technique, for a uniform temporal sampling – as in our case – may give too pessimistic estimates of errors (this seems to be actually the case, as seen in Fig. 3), but we prefer this conservative approach. The amplitude $a(f)$ for each frequency was evaluated as the modulus of the periodic component, $a(f) = \sqrt{c_1(f)^2 + c_2(f)^2}$. Because of the continuing changes in the spectrum (see further in this paper), the phase information was disregarded except for a comparison with the contemporaneous radial-velocity observations, as described below in Section 4.3

The amplitude spectrum is shown in Fig. 2. In this spectrum, all components with frequencies <2 c d^{-1} (periods longer than half a day) appear to be significant and real. In agreement with what was noted in Fig. 1, we see an obvious periodic signal at 0.27 ± 0.007 c d^{-1} which corresponds to a period of 3.7 ± 0.1 d. Because the data series were only 11 d long, we could not establish the period more accurately, but it is consistent with the periodic signal of 3.56 d

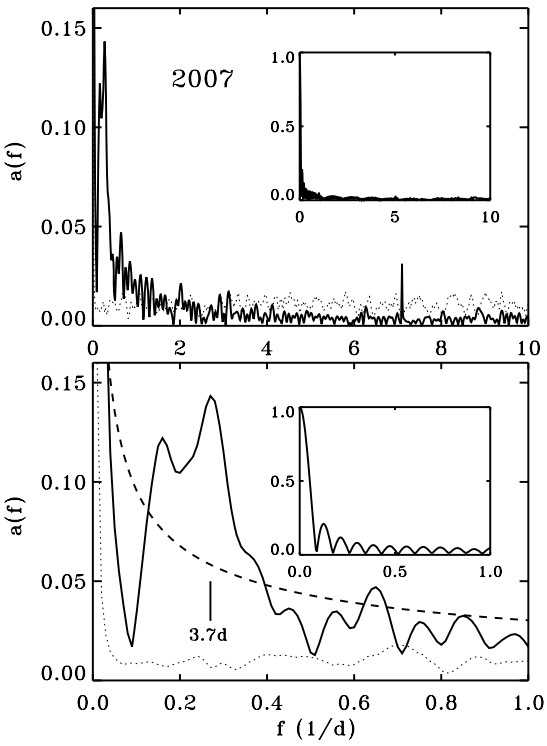

Figure 2. The frequency spectrum expressed in amplitudes for the MOST 2007 data at frequencies below 10 c d^{-1} (the upper panel) and up to 1 c d^{-1} (the lower panel). The mean standard errors of the amplitudes, as estimated by the bootstrap sampling technique, are given by the thin, dotted line. Note that the downward drift of the mean brightness level through the observing run has resulted in a large amplitude at the lowest frequencies. The broken line shows the arbitrarily scaled $a \propto 1/\sqrt{f}$ dependence. This line is repeated in other similar figures later on, particularly in Fig. 3 where it appears as the upper broken straight line. Because of the practically uniform temporal sampling (only two data points missing in 163 consecutive MOST orbits), the spectral window is exceptionally clean and its side lobes are very small.

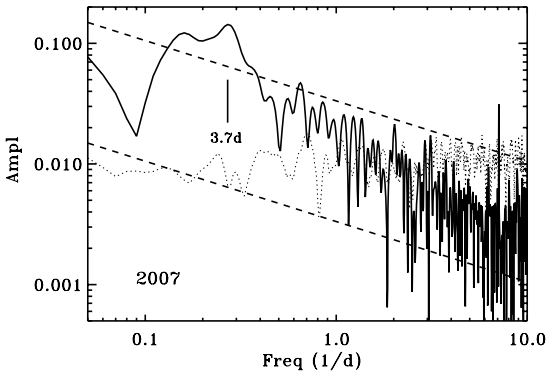

Figure 3. The frequency spectrum expressed in amplitudes for the MOST 2007 data of TW Hya, plotted in log–log units. The broken lines give the slope of 'flicker' noise, $a \propto 1/\sqrt{f}$, whereas the thin, dotted line gives the approximate mean standard errors of the amplitudes.

in the radial-velocity data, as discovered by Setiawan et al. (2008). Because of the limited duration of the run, we also consider the next peak in the frequency spectrum corresponding to a 6.2 d period as non-physical. It should be noted that no variability appears with any of the several periods listed in Section 3; in particular, the period close to 2.1 d, which was suggested as the stellar rotation time-scale by Setiawan et al. (2008) is not visible at all.

In Fig. 3, we show the same amplitude spectrum as in Fig. 2, but in the log–log units. The spectrum clearly rises at low frequencies in a way which is characteristic for 'red noise'. As described lucidly by Press (1978), the special type of red noise, called 'flicker noise', with amplitude spectrum $a(f) \propto 1/\sqrt{f}$ (i.e. the power $\propto 1/f$) is very common and appears in various circumstances, although it is not clear why it is so prevalent in nature. Although, strictly speaking, the variability power diverges at low frequencies and is non-integrable, there usually exists a low frequency limit set by the slowest permissible response of the given dynamical system.

The strong 3.7 d signal in the 2007 MOST data appears to define the lowest frequency periodicity, although we note that the overall brightness of the star drifted down during the span of 11 d. The 3.7 d periodicity was stronger than estimated from a simple extrapolation of the flicker noise from the range of moderately high frequencies of 0.7–5 c d^{-1} into the low-frequency end, to < 0.5 c d^{-1}.

4.3 The 3.7 d photometric and the 3.56 d spectroscopic periodicities: the same thing?

Attempts at an analysis of the 2007 data using wavelets and fractal techniques (see the description for the 2008 data, Section 5.3) showed that the 2007 run was simply too short to state anything beyond the existence of the very clear 3.7 d periodicity, superimposed on (or as part of) a more complex flicker-noise variability. In fact, in view of this particular type of variability, even the 3.7 d periodicity may be considered questionable in view of the remark of Press (1978) that any period equal to 1/3 of the length of the flicker-noise dominated data is probably spurious. If not for the presence of the 3.56 d periodicity observed at the exactly same time, in the very differently obtained radial-velocity data of Setiawan et al. (2008), one would be tempted to interpret the 3.7 d period as an exceptionally large flicker-noise 'fluke'.

The 2007 MOST run was located between the two sections of the Setiawan et al. (2008) radial-velocity observations which had a gap of 1.5 months between *HJD* $-$ 2 450 000 d 4172 and 4215.

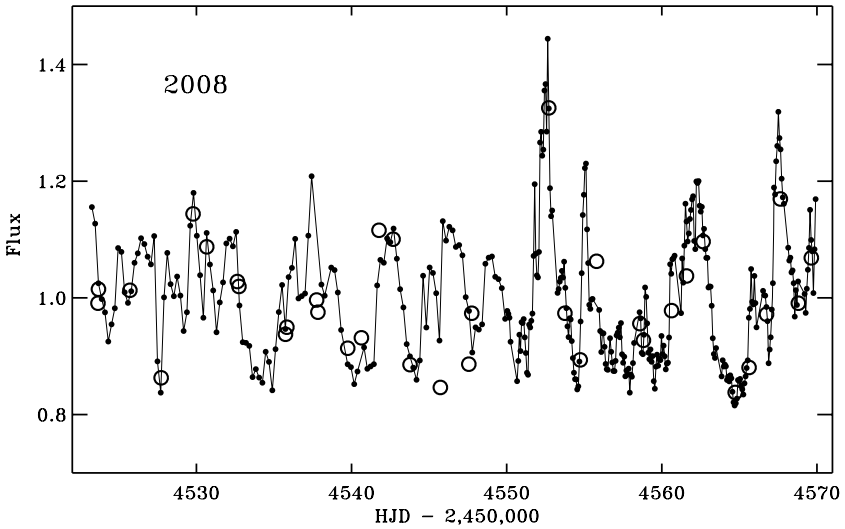

Figure 4. MOST observations of TW Hya in 2008 with observations binned into mean points, separated by the intervals of (small) multiples of the satellite orbital period of 0.0705 d. Until day 4550, the data points are separated by typically two to three satellite orbits; after that, the sampling became denser at every one to two satellite orbits with regular (every 2.6 d), widely spaced gaps of four to five orbits. Note that the *Y*-scale of this figure is the same as in Fig. 1, although the 2007 and 2008 mean flux levels were separately normalized and cannot be directly compared. Note also that the transformed to intensities, ASAS *V*-band observations (large, open circles) are plotted here with the same assumed reference level ($\bar{V} = 11.04$; see Section 6).

Apparently, the radial-velocity variations kept the same phase through the duration of this gap so that one can plot the interpolated radial-velocity changes for the dates of the MOST observations. To do that, the phase information for the Setiawan et al. (2008) data has been restored from the original radial-velocity observations and the expected variations plotted in the lower panel of Fig. 1. The results are very important for the interpretation of the 3.56/3.7 d periodicity: the photometric and spectroscopic observations were synchronized in such a way that the largest radial-velocity excursions occurred at the time of the fastest brightness changes, i.e. the two types of variation were shifted in phase by 90°. Thus, for the orbital motion of a planet or of a gas blob inside the disc, the photometric extreme values were reached during what (in binary star language) would be called the 'conjunctions': the star was brightest when the radial velocity went through the zero deviation, when switching for the approach to the recession part of the cycle (the planet/blob in front the star), and was faintest when the radial velocity went through the zero deviation from the recession to the approach (the planet/blob behind). This type of the phase relation would agree with the spot explanation, but – if the star is really seen pole-on – the spot modulation is expected to be small and could not lead to the observed brightness variations by 30–40 per cent.

5 MOST 2008 OBSERVATIONS

5.1 The data

MOST observed TW Hya the second time for 46.7 d from 2008 February 26 to April 13. All remaining details of the observations were the same as for the 2007 run except that: (i) the switch targets were different, HD 99563 during the first month and HD 102195 for the last 17 d, (ii) the star was observed typically every second or third MOST orbit and (iii) during the period of March 24 to April 12, the TW Hya observations were interrupted for five to seven satellite orbits every 2.6 d. These restrictions resulted in larger gaps in observations than in 2007, but the gaps did not affect the low variability frequencies which are the main target of our interest.

The 2008 data are listed in Table 1 and shown in Fig. 4. Note that the 2007 and 2008 fluxes have been separately normalized because of (possible) small differences in the satellite sensitivity precluded direct ties of the 2007 and 2008 seasonal mean levels. However, the ground-based *V*-band data do not indicate any large change in the mean light level; see Section 6, where the variability of TW Hya over time-scales of months and years is analysed.

The individual MOST-orbit observations lasted between 12 and 33 min and were typically spaced by small multiples of the satellite orbital period of 101.4 min. The formal errors per mean satellite-orbit point have the median of 0.0018 of the mean flux level and the range of 0.001–0.005, with a small number of relatively poorer observations having uncertainties approaching 0.007.

The general characteristics of the 2008 TW Hya variability are the same as in the 2007 observations, but we clearly see and can follow much more activity in such a long data series. Brightness increases appear to be more common than dimming events. This is visible directly in Fig. 4 and through the skewness (+0.772) of the distribution of the deviations from the mean level (Fig. 5), where upward spikes produce a positive tail in the distribution.[1]

5.2 Fourier analysis of the 2008 time series

The Fourier analysis of the 2008 data was done exactly in the same way as for the 2007 data. The same relatively dense frequency sampling of $\Delta f = 0.01$ was used which was more appropriate than in 2007 in view of the longer duration of the run.

The figure (Fig. 6) is now very different from that in 2007: the strong 3.7 d periodicity, so well defined in the 2007 run, is entirely absent. Instead, a number of periodic components with slightly smaller amplitudes than the 2007 periodicity appear to be present at $f < 1$ c d^{-1}, their formally derived periods are 7.7, 5.1, 3.3,

[1] We have not performed this exercise for the 2007 data because this would require to remove the slow changes which do not have a clear interpretation or description.

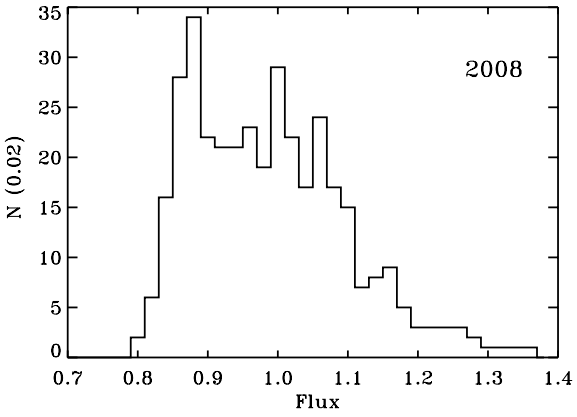

Figure 5. The distribution of deviations from the mean flux level for the MOST 2008 data indicating the presence of relatively short lasting spikes superimposed on a moderately steady background level.

2.5, 1.74 and 1.25 d. Note that all are very highly significant as the comparison of the amplitudes with their errors in Fig. 6 clearly shows. Their amplitude progression indicates a modulation by an envelope $\propto 1/\sqrt{f}$, that is again pointing to flicker noise. The feature at $f \simeq 4.5$–5 c d^{-1} (0.21–0.22 d) appears in the spectral window and is an artefact of the gaps in the data occurring at the spacing of 3 times the satellite period. The spectral window is however relatively 'clean' in the low-frequency range ($0 < f < 1$ c d^{-1}) so that all components visible in the lower panel of Fig. 6 are real and well defined.

The log–log plot (Fig. 7) confirms the flicker-noise amplitude distribution. The slope seems to be locally slightly steeper in the range $0.15 < f < 1.5$ c d^{-1} (periods $\simeq 0.7 < P < 7$ d) as if slower variations were a bit more likely to appear than for the strict flicker noise. Viewed in this light, the 3.7 d variability observed in 2007 could be an extreme manifestation of this tendency.

5.3 Wavelet analysis of the 2008 time series

The Fourier analysis presented in Sections 4.2 and 5.2 addresses the periodic content in the TW Hya variability. But, from the comparison of the 2007 and 2008 data, we know that the periods of the variability must change in time. While Fourier analysis cannot trace such temporal changes, the wavelet technique has been developed specifically as a tool to localize in time finite wave trains of various periodicities and durations. Extensive literature on the subject exists; of particular use to us was Torrence & Compo (1998) following the ideas developed in the seminal work of Daubechies (1992).

The wavelet and fractal (the next Section) analyses require the data to be spaced uniformly in time. To achieve this time uniformity, the 2008 MOST data have been mapped into a strict equidistant grid of points spaced at 0.07047 d (the satellite revolution period) using splines. Deviations of the actual observations from uniformity of the time-scale were small, typically 1–2 min. However, because of the different satellite target switching, gaps lasting typically two or three satellite orbits occurred. The spline interpolation into the uniform scale resulted in 663 points spanning the same time range as the original data.

The 2008 data were subjected to wavelet analysis using several different types of wavelet functions. The best and most clearly defined results were obtained with the simplest (sometimes considered the 'natural') Morlet, complex wavelet consisting of a coupled sine–cosine pair modulated by a Gaussian function.

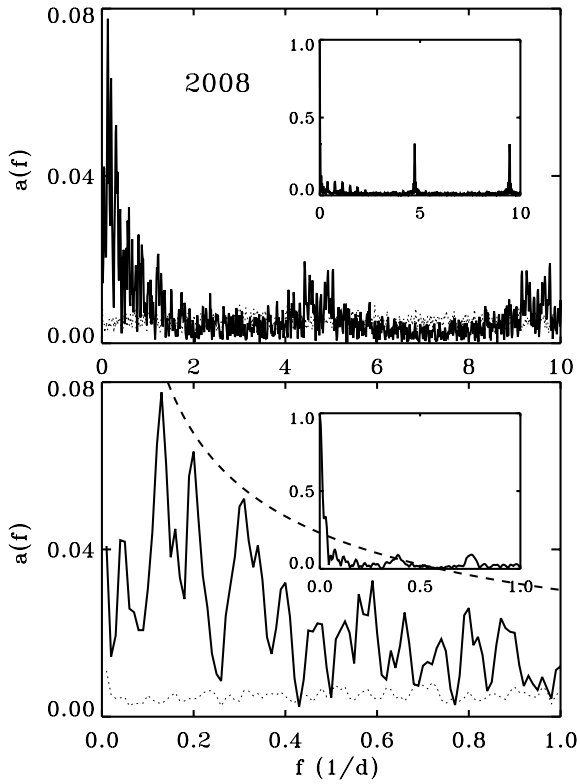

Figure 6. The frequency spectrum expressed in amplitudes for the MOST 2008 data, for frequencies up to 10 c d^{-1} (the upper panel) and up to 1 c d^{-1} (the lower panel). Compare this with Fig. 2 and note that the amplitudes are smaller than in 2007 so that the vertical scale is reduced here by a factor of 2. The broken line shows the arbitrarily scaled $1/\sqrt{f}$ dependence; it is the same upper envelope as in Figs 2, 3 and 7. The inserts show the spectral window. Note that it is not as 'clean' as for the 2007 observations because only 364 of 663 consecutive MOST orbits were used, with the most common spacing of three satellite orbits.

The wavelet power (the squared modulus of the transform) for the 2008 observations of TW Hya is shown in Fig. 8. We do not address the matter of units of the power[2] and utilize only the periods and the time localization of the periodic wave packets. The wavelet transform was calculated with the usual power-law time-scale progression (1, 2, 4, 8 . . . data point spacing) but for the ease of viewing and interpretation, the transform has been interpolated into a linear time-scale. In the grey-scale image, a single bright spot corresponds to a well-defined periodic packet which lasts about five to six oscillation periods while any horizontal widening of it would indicate a longer duration of the periodic wave.

The results of the wavelet analysis of the TW Hya MOST data (Fig. 8) are striking and very important: periodic oscillations apparently appeared at some periods, lasted for some time and died out. During their lifetimes, they had a tendency to shorten the period. In particular, a periodic variation with a period of about 5–6 d started around the day $t \simeq 4530$–4533 and rapidly shortened its period to about 3 d in some 10 d; possibly, the isolated 2.5 d periodicity appearing later around day 4553 is actually an extension of this progression. Another periodic variation started at about day 4550–4552 with a period of about 7 d, became very strong at about the day 4560 evolving into a wider, less concentrated feature of a slightly

[2] We used the routine 'wv_cwt' in the IDL 6.3 software to calculate the power of the wavelet components.

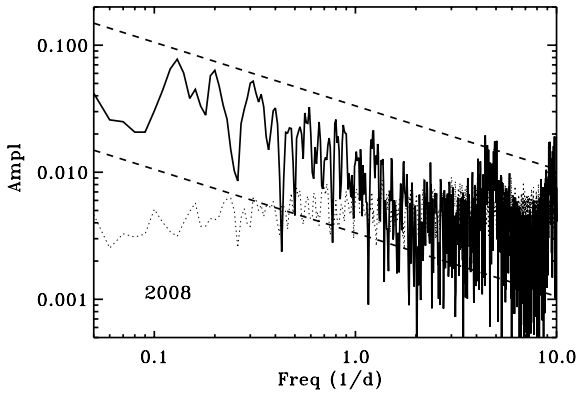

Figure 7. The frequency spectrum expressed in amplitudes for the 2008 MOST data of TW Hya plotted in log–log units. The broken lines give the slope of the 'flicker' noise, $a \propto 1/\sqrt{f}$, whereas the thin, dotted line gives the approximate mean standard errors of the amplitudes. The vertical scale is the same as in Fig. 3 so one can see here the absence of the strong 3.7 d periodicity.

shorter period; it could not be followed further because of the end of the data.

Although our analysis extended to both, short ($P \geq 0.2$ d) as well as long ($P \leq 20$ d) periods, there is no indication of any periodic activity outside of the range of $2 < P < 9$ d. This very well agrees with the Fourier analyses presented before and suggests a rather well-defined range of temporal scales. At a given time usually only one periodicity was present. The several spectral features in Fig. 6 with frequencies >0.5 c d^{-1} are most probably harmonic artefacts of single wave trains changing their periods. As noted in the description of the Fourier analysis (Section 5.2), we see no trace of any dominant periodicity with a period of 3.5–3.7 d. Thus, the strong signal in the 2007 data was entirely absent in the 2008 observations.

A comment is necessary here about the assumed duration or the 'order' of the Morlet wavelet analysing function. In the literature, the order of the Morlet wavelet packet is frequently not explicitly given, but appears to be usually assumed to describe five sine–cosine cycles per one Gaussian-enveloped packet. An attempt was made to utilize the Morlet wavelets of different orders to find the optimum fit to the *duration of the wave packet, expressed in the number of periods*. Unfortunately, we found a unexpected problem: in the wavelet analysis, there appears to exist a coupling between the duration of the packet (the length of the Gaussian envelope) and the oscillation period. In other words, a packet will show a slightly different period depending on the assumed order. As a result, for different orders, the whole two-dimensional wavelet transform structure, as in Fig. 8, is stretched or compressed vertically depending on the order. We were able to remove this arbitrariness by imposing the condition that the time-averaged power distribution (the right-hand side of that figure) has the same shape as the Fourier spectrum power. Using this principle, we found that Morlet-6, and not Morlet-5, is the most appropriate. Further tests on artificial data for the Morlet orders four to seven showed that a typical shift in the period scale is about 20 per cent per increment in the wavelet order. This property does not seem to be widely known or described but it appears to be a limitation of the wavelet approach. It precludes our original hopes of the evaluation of how many cycles are confined in a typical wave packet for TW Hya.

Very similar results with similar time-scales (periods) and wave-packet localizations as for Morlet-6 were obtained for the 2008 data with another popular wavelet function, the Paul-4 wavelet. However, an application of the wavelet analysis to the 2007 data has not led to any new results: the main 3.7 d single periodicity dominated the picture, its amplitude diminished through the 11 d MOST sequence

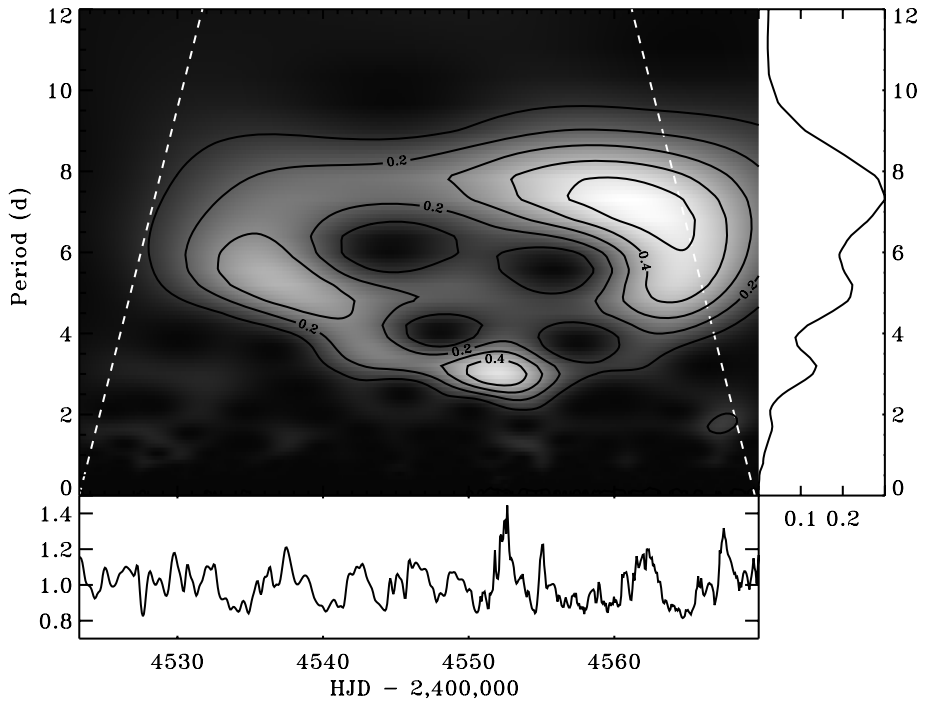

Figure 8. The Morlet wavelet transform of the 2008 MOST data. The grey-scale gives the power of the transform. The edge effects are present beyond the white, slanted, broken lines. The TW Hya brightness data, re-sampled into a uniform grid with time-point spacing of 0.07 d are shown at the bottom. The projected mean frequency spectrum is shown at the right margin; compare with Fig. 6, but note the poorer definition of the spectrum here, the price paid for localization of the periodic events.

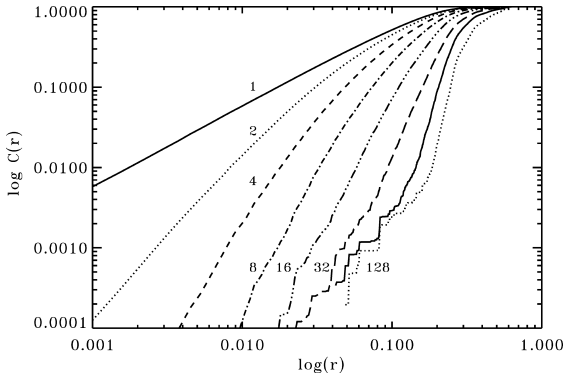

Figure 9. The fractal properties of the 2008 MOST data of TW Hya analysed using the correlation integral $C(r)$. The line labels (powers of 2) give the lengths of segments used in the calculation of $C(r)$; they can be converted into the time-scale lengths by multiplying them by the length of the data spacing of 0.07047 d. For definitions and conventions, see the cited literature, in particular Lehto et al. (1993).

so that the formally derived single-period wavelet had a maximum in the first part of the run.

5.4 Fractal analysis of the 2008 time series

An attempt to analyse the irregular photometric variability of TW Hya for any indications of a deterministic process was made. The same 2008 time series as the one described above in the wavelet analysis and consisting of 663 equidistant points were used here. The fractal technique utilized the correlation integral, first described by Grassberger & Procaccia (1983) and studied extensively in Voges et al. (1987) and Lehto, Czerny & McHardy (1993). This approach may – in some circumstances – permit evaluation of the fractal dimension (if such can be defined) and may reveal the type of variability. The data are sampled in segments of progressively larger length and 'distances' are calculated between all pairs of such segments, then the number of pairs satisfying a criterion of the distance is found. For the description of the terms and definitions used in this technique, The reader is directed to the paper of Lehto et al. (1993).

In Fig. 9, we see that the formally derived dimension [from the logarithmic slope of the correlation integral $C(r)$ versus the distance of the points, r] is not unique and increases with the size of the embedded dimension d in the range of 1–32 data intervals, that is in the time-scales of 0.07–2.2 d. As discussed by Lehto et al. (1993), this is a property characteristic for independent, uncorrelated shot-noise events. Beyond the point of the time-scales corresponding to $\simeq 2$ d, the correlation integral changes its character, and a ragged structure in $C(r)$ becomes visible for the time-scales of 2–9 d. This structure appears to be related to the semiregular variability so clearly manifested in the wavelet analysis. This result fully confirms lack of any periodic events in the wavelet analysis for time-scales <2 d.

6 ASAS OBSERVATIONS

6.1 The ASAS data

ASAS (Pojmański 1997, 2002, 2004; Pojmański & Maciejewski 2005; Paczyński et al. 2006)[3] is a long-term project dedicated to detection and monitoring of variability of bright stars using small telescopes. It has been run by the Warsaw University at the Las Campanas Observatory in Chile using 7 cm telescopes providing the best photometry in the 8–13 mag range. About three-fourths of the sky (the southern and equatorial parts, with $-90^\circ < \delta < +28^\circ$) have been monitored for stellar variability in V and I filters. The typical random errors are at the level of 0.01–0.02 mag. The high stability of the system and of the photometric reductions and calibrations results in a very consistent data set.

[3] See: http://www.astrouw.edu.pl/∼gp/asas/asas.html and http://archive.princeton.edu/∼asas/

Table 2. ASAS photometric data for TW Hya, 2001–2008. The whole table is available on-line only.

(1) t	(2) V/I	(3) Error	(4) Filter
2405.5505	9.341	0.063	I
2406.5620	9.374	0.062	I
2415.5269	9.305	0.061	I
2619.7858	9.378	0.058	I
2619.8205	9.387	0.060	I

The columns: (1) the time, $t = JD - 2\,450\,000$; (2) the magnitude in the V or I filters; (3) an estimate of the mean error of the magnitude provided by the ASAS project; it should be taken in the relative sense, in comparison between observations and is usually an over-estimate; (4) the filter used, I or V.

The ASAS observations of TW Hya analysed here cover 8-yr seasons, 2001–2008, centred on late February of each year (Table 2). The photometric observations are plotted versus the HJD in Fig. 10. As was noticed before by Rucinski & Krautter (1983), (i) the variability in the V band is much stronger than in the I band, (ii) the $V - I$ colour index changes follow the V changes so that the V-band variations are larger and easier to study than the I band ones. Note that with $\bar{V} \simeq 11.0$ and $\bar{I} \simeq 9.3$, TW Hya is an easy object for ASAS. The measurement errors in both bands are similar, at the level of 0.01–0.02 mag, and reflect mostly the uncertainties in the standard system transformations over large ASAS fields.

While the night-to-night variability of TW Hya appears as random scatter in Fig. 10, the seasonal data show well-defined slow changes with $\Delta V = 0.18$, from $V = 11.05$ in 2003 to $V = 10.87$ in 2006 and by $\Delta I = 0.06$, from $I = 9.36$ in 2003 to $I = 9.30$ in 2006. Twenty years earlier, in 1982 (Rucinski & Krautter 1983), the star was slightly fainter with mean $V \simeq 11.15$ and $I \simeq 9.5$, but the night-to-night variability ranges were similar, with $\Delta V \simeq 0.35$ and $\Delta I \simeq 0.15$.

6.2 Fourier analysis of the whole data set

Because the I band variability of TW Hya appears to follow the V band variability but with reduced scale, we present here periodic analysis of the V data only. We should note that the V variability cannot be directly compared with that observed by MOST. The MOST single filter is located red ward of the V-band effective wavelength, so that the V-band amplitudes of TW Hya are expected to be slightly larger than the MOST amplitudes.

The whole span of the ASAS observations extends over about 3000 d setting a limit to the lowest detectable frequencies of 0.0003 c d^{-1}. We consider here the frequencies up to 0.5 c d^{-1} which would be accessible for the one-day sampling. In fact, the most frequent data spacing was 2 d, it occurred for 43 per cent of the V observations and 51 per cent of the I observations. A smaller number of observations were spaced by 1 d, 17 per cent of V and 10 per cent of I observations, and 5 and 7 per cent of all V and I

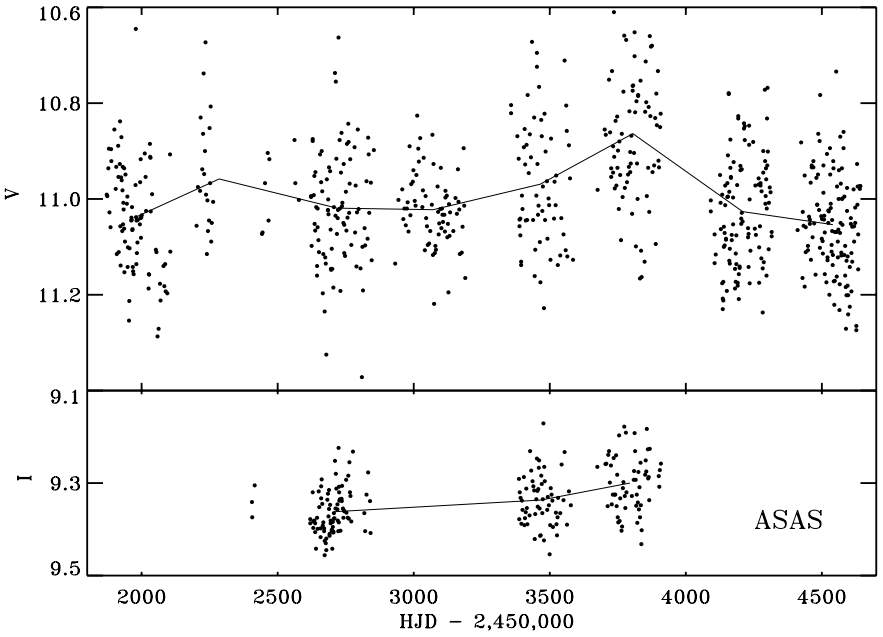

Figure 10. The ASAS data for TW Hya in *V* and *I* band filters in eight consecutive observing seasons, 2001–2008. Most of the scatter is due to variability of TW Hya; the observational errors in both filters are at the level of 0.01–0.02 mag. The lines connect the mean seasonal values of the magnitudes.

observations were done twice on a given night. The resulting spectral window is relatively simple (Fig. 11) and shows only the yearly signal at 0.00274 c d^{-1} and a feature at 0.0677 c d^{-1} corresponding to the time-scale of 148 d, somewhat similar to the duration of each seasonal run.

The frequency analysis of the ASAS data was done in the same way as described in Section 4.2, through least-squares fits and bootstrap-error estimates. The bootstrap technique is particularly useful here because of the unequal temporal distribution of the data. In the analysis of the full *V* band ASAS data set, the seasonal trends were *not removed* to retain the low-frequency component of the variability. While the spectrum expressed in linear units is featureless, indicating lack of coherence over 8 yr. Fig. 12 shows that, in the wide range of frequencies of 0.0001–0.5 c d^{-1}, the spectrum approximately follows a 'flicker-noise' dependence. The seasonal mean-level changes are apparently part of this picture. Because of the long extent of the ASAS data, the low frequencies are very well defined, in spite of the ASAS *V*-amplitude errors at the level of $\sigma_a \simeq 0.01$–0.02. At higher frequencies accessible to MOST observations ($f > 0.02$ c d^{-1}), the MOST results are far superior over the ASAS ones, mostly because of the amplitude errors by an order of magnitude smaller than for ASAS (see Fig. 7).

The maxima along the low-frequency 'flicker-noise' progression, in Fig. 12, corresponding to periods of 155, 317 and 510 d appear to be significant ($>3\sigma$), but their reality is not fully established. In the frequency range of $0.05 < f < 0.5$ c d^{-1} (time-scales 2–20 d), the observational noise with similar amplitudes $a \simeq 0.01$ dominates the spectrum. Within this range, the spectrum contains many formally significant periodicities with amplitudes $\geq 4\sigma$ (but none of $\geq 5\sigma$). However, in view of the MOST 2008 results, it appears that some oscillation power extends throughout the whole spectrum accessible from the *V* data ($0.0003 < f < 0.5$ c d^{-1}), but none was coherent enough to produce a single peak to be detectable in the ASAS observations.

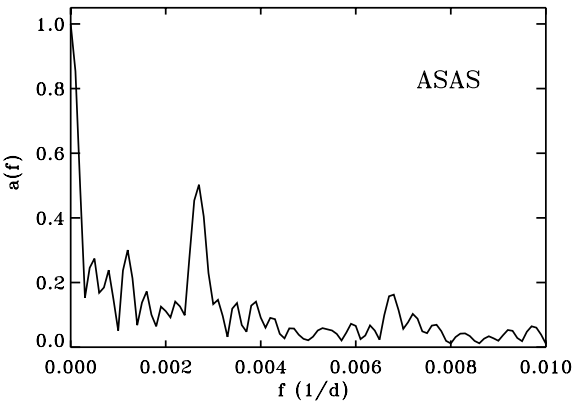

Figure 11. The spectral window for all *V*-band ASAS observations of TW Hya during the 2001–2008 seasons. The window is free of any features at frequencies higher than shown in the figure.

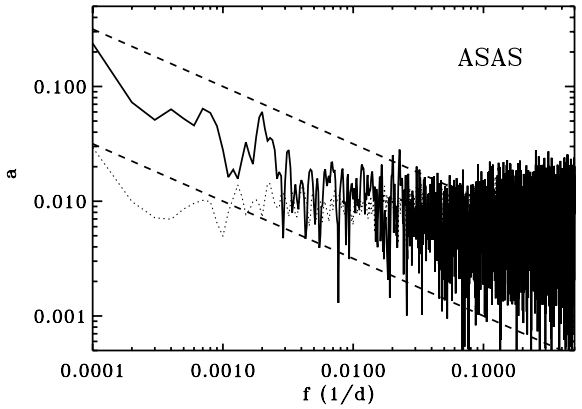

Figure 12. The amplitude frequency spectrum for all *V*-band ASAS data of TW Hya of the 2001–2008 seasons, plotted in log–log units. The broken lines give the slope of flicker noise, $a \propto 1/\sqrt{f}$, whereas the thin, dotted line gives the approximate mean standard errors of the amplitudes.

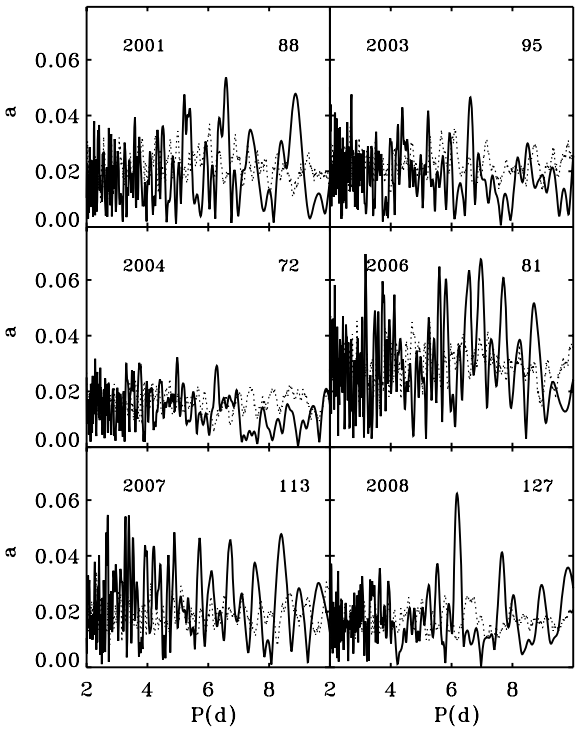

Figure 13. The period analysis of the seasonal ASAS data in the *V* band for TW Hya for the six best observed periods, in the period range of 2–10 d only. The mean standard error level in each panel is given by the thin, dotted line. The numbers identify the year and give the number of observations.

6.3 Fourier analysis of the seasonal data

In order to find periodic variability during individual seasons, the ASAS *V*-band data were analysed with the seasonal mean brightness levels subtracted. Such data may give better defined results than a search for periodicities in the combined ASAS data set because (i) the low frequency, interseasonal variation is apparently strong and may influence results for the shorter time-scales, and (ii) the MOST results suggest short duration of individual oscillations of only a few oscillation periods.

The seasonal ASAS runs lasted typically 150–250 d each year (i.e. some three to five times longer than the 2008 MOST run) and consisted of 27–127 observations. The two last seasons, 2007 and 2008, which are most important for a comparison with the MOST data, were the best observed with 113 and 127 observations, respectively. The lowest frequencies accessible from the seasonal data sets are $\simeq 0.005$ c d^{-1}.

The results are presented in the form of period – amplitude spectra (Fig. 13) for the six seasons which had more than 70 observations per season. For the best presentation, only the period range of 2–10 d is shown and the spectra are expressed versus the period rather than the frequency. This is the range where very well-defined semiperiodic variability was observed by MOST in 2007 and 2008, we address the matter of the ASAS observations during the MOST runs in the next section.

6.4 ASAS observations during the 2007 and 2008 MOST runs

A comparison of the ASAS and MOST results cannot be done directly because the ASAS data extended for typically about 200 d during each season, while the MOST runs were comparatively short, of 11 and 46 d. Also, the ASAS observations were done at intervals of typically 2 d, sometimes even 3–5 d, as can be seen in the distribution of large circles among the MOST observations in Figs 1 and 4. Note that in these figures, the *V*-band observations were arbitrarily adjusted to the assumed mean level of $\bar{V} = 11.04$ while the difference in the expected variation amplitudes between the *V* band and the MOST band (between *R* and *I*) was disregarded.

We notice in Fig. 13 that the ASAS 2008 season data show a single, strong, well-defined periodicity of 6.18 d (0.162 c d^{-1}). Surprisingly, it is entirely absent in the MOST 2008 spectrum (see Fig. 2), the nearest peaks are at 7.8 and 5.0 d (the second ASAS periodicity of 7.67 d may be identical with the 7.8 d MOST period). This behaviour is very typical for all ASAS seasons: some periodic, coherent variations appear at various frequencies (usually never the same), but their amplitudes are not as well defined as in the MOST data and they do not directly show any 'flicker noise', $a \propto 1/\sqrt{f}$ characteristics. We suspect that the irregular spacing of the ASAS observations was the reason for the latter effect.

A comparison for the 2007 season is most interesting as during this time the well-defined periodicities were observed photometrically (MOST, 3.7 d) and in radial velocities [3.56 d; Setiawan et al. (2008)], within the period uncertainty, this is the same variation showing a simple phase relation between the two observables (Section 4.3). Unfortunately, only five ASAS observations were obtained during the 2007 MOST run, but they show the perfect consistency of the ASAS and MOST observations (see Fig. 1). However, 45 ASAS observations happened to fall into the full extent of the radial-velocity observations (Setiawan et al. 2008). In Fig. 14, we compare the full results for the 2007 season ASAS observations with the subset obtained during the time when the radial-velocity

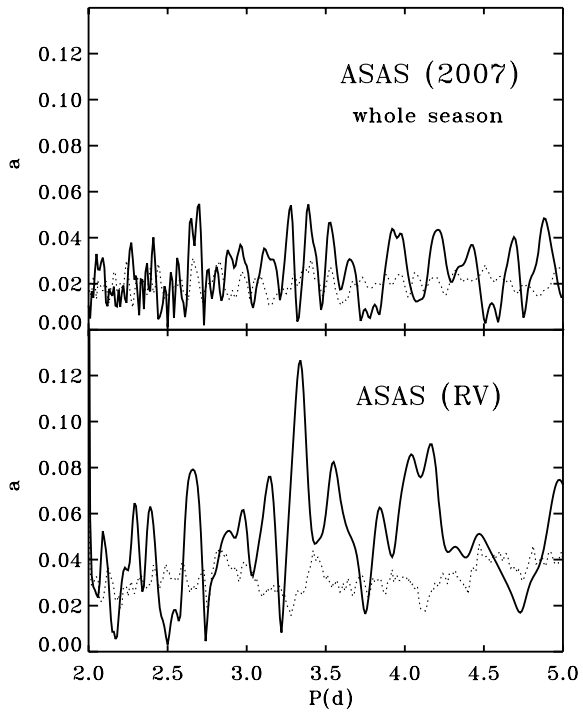

Figure 14. The period analysis of the seasonal ASAS data in *V* for TW Hya for the whole 2007 season in the period range where the strong periodicity was observed by MOST is shown in the upper panel. The dotted line gives the errors of amplitudes. The analysis of the reduced set of the ASAS data, obtained within the duration of the radial-velocity observations of Setiawan et al. (2008) is shown in the lower panel.

observations revealed the very strong 3.56 d periodicity. As we can see in Fig. 14, the longer ASAS 2007 data set gives smaller amplitudes, indicating a loss of coherency. Very clear periodicities are visible in the reduced-duration data set, but none corresponds to $\simeq$3.56 d. However, this may be due to the irregular data sampling in the ASAS project because significant periodicities appear at 3.3 and 4.1 d.

Thus, the ASAS data are very useful for an extension of the frequency spectrum to very low frequencies beyond the limit of the MOST data (as set by the duration of the 2008 run), but the picture obtained for the seasonal ASAS runs is confusing and would certainly not lead to such clear-cut results as from the MOST data. The ASAS project, with its irregular sampling, could not detect single, but variable periodicities because of the obvious loss of coherence. But variability is definitely there, only one cannot characterize it as well as for the MOST data.

7 SUMMARY AND DISCUSSION

Our analysis of TW Hya contributes substantially to the knowledge of T Tauri type photometric variability. Although connection with the stellar rotation cannot be directly demonstrated, the MOST observations are phenomenologically consistent with the Type IIp variability of TW Hya, as suggested by Herbst et al. (1994). The great advantage of the MOST observations was their continuous and uniform time coverage of 11 d in 2007 and 46 d in 2008, both sampled at the satellite-orbit interval of 0.07 d. The ASAS observations permitted extension of the time-scale coverage to $\simeq$3000 d but with irregular and sparse sampling at typically 1–5 d.

During the 2007 MOST observations, a single, strong 3.7 d period dominated the brightness changes. This variation had a similar period to the 3.56 d radial-velocity variation with semi-amplitude of 200 m s^{-1} observed at the same time by Setiawan et al. (2008). The phase relation between the two phenomena was such that the originally offered explanation of an orbiting planet has great difficulty in explaining the observations: only a single (per orbit) brightness maximum took place at what – for the orbital revolution hypothesis – would be interpreted as inferior conjunction of the planet. While this phase relation could result from a spot modulation, the presumed low inclination angle of the rotation axis makes this hypothesis very unlikely. We note that this periodicity did not show up directly in the ASAS observations during the 2007 season, but the reason for that may be in the irregular ASAS data sampling.

The 3.56/3.7 d periodic modulation did not re-appear in the four-times longer MOST run of 2008. All changes during this run can be interpreted as semiperiodic events (mostly brightening spikes) superimposed on a baseline level. Several Fourier components appeared at periods ranging between 1.2 and 7.7 d with noticeably smaller amplitudes than the 2007 periodicity, they had progressively smaller amplitudes with decreasing periods with an envelope suggesting flicker-noise properties. The long MOST 2008 run, analysed with wavelets for the period range $0.2 < P < 20$ d, showed discrete periods subject to a well-defined period-change pattern: all variations were monoperiodic, appeared in the 2–9 d range, changed their periods, lasted a few cycles and then died out. An evolution of the period from $\simeq$5–6 to $\simeq$3 d in the time-scale of about 10 d was observed. Thus, the Fourier components showing that flicker-noise amplitude distribution appeared to be another representation of the monoperiodic features evolving within the 2–9 d period range. No wavelet-detectable components were seen for time-scales >9 d nor for the $0.2 < P < 2$ d range, with the latter range being dominated by small, shot-noise events.

The variability of TW Hya is most likely powered by accretion phenomena in its disc. Because of the low inclination of the rotation axis, the disc is visible almost face on with its inner parts exposed. The star inside the disc is relatively small; it has the radius $\simeq$1 R$_\odot$, that is only slightly larger than a main-sequence star of the same spectral type. This can be estimated using the *Hipparcos* distance $d = 56$ pc and the faintest level ever observed, $V \simeq 11.3$ (Rucinski & Krautter 1983), hence the luminosity of the 'naked' star is expected to be $M_V \simeq 7.56$. For comparison, a main-sequence K5V star would have $M_V \simeq 7.8$, while a K7V star would have $M_V \simeq 8.1$. Thus, the small overluminosity may be interpreted by a radius excess of 12–28 per cent over the main-sequence value.

The Keplerian orbits for a 0.72 M$_\odot$ star [for consistency, we assume the same mass as in Setiawan et al. (2008)] with periods 2, 4 and 8 d would be located at the disc radii of 6, 9.5 and 15 R$_\odot$. These may be the locations where bright, hot patches or blobs of changing optical depth formed and remained stable for a few orbital revolutions. Although we do not know the exact mechanism, and we cannot disentangle separate contributions from the changing area, optical depth or temperature, we suspect that the latter dominates because of the strong brightness – colour correlation in the variations observed before (Rucinski & Krautter 1983). TW Hya definitely requires a well-organized observational effort, involving spectroscopy supporting further MOST satellite observations.

Big questions remain: the rotation period of TW Hya is still unknown; the previously suggested value of about 2 d is just a plausible guess. We also have no interpretation or mechanism for the strong 2007 periodicity. The brightness variations with the shortening periods observed in 2008 are unexplained but it is virtually impossible to explain all these phenomena by surface spots. Large, optically thick, hot-plasma structures and anchored in different parts of the inner accretion disc would be better candidates. They could extend to large latitudes and explain the brightness variations through changes in their optical depth even for a low rotational inclination angle.

8 CONCLUSIONS

Following our analysis of the MOST and ASAS very different but partly complementary observational data sets, and considering conclusions of the important paper by Press (1978) on the common occurrence of flicker noise (with Fourier amplitudes scaling as $a \propto 1/\sqrt{f}$), we cannot resist a comparison of the TW Hya photometric variability with an orchestra. As pointed out by Press (1978), the spectrum of the orchestra sound can be usually described by the prosaic flicker noise. Thus, although we hear the music defined by an entire orchestra where everybody plays a different piece, sometimes the melody (tune) produced by an individual instrument becomes notable against the general flicker-noise level. We observed such distinct, time-variable 'tones' in the period range of 2–9 d; they may be manifestations of the accretion process as the matter spirals into the star.

The flicker-noise spectrum of TW Hya photometric variations appears to extend from very low frequency of 0.0003 c d^{-1} (accessible from 8 yr of the ASAS data) to $\simeq$10 c d^{-1} (accessible to our MOST observations). The lowest frequencies require long monitoring time, so that good photometric stability and consistency of calibrations are essential, even at relatively moderate accuracy (0.01–0.02 mag) of the ASAS project. At frequencies corresponding to days to weeks, the uniform time coverage and high accuracy of the MOST mission (0.003–0.005 mag, even with the included intrinsic variability of the star in times scales shorter than an hour) permitted us to study the

difficult (from the ground) frequency range of $\simeq$0.025–10 c d^{-1}. In this range, we observed very clear, well defined, varying 'tones' in the 0.1–1.0 c d^{-1} range only (specifically, the variable periods within 2–9 d). It would be tempting to identify those changing periods as signatures of the orbital decay as the accreting material spirals into the star. The strong periodicity observed by MOST in 2007 with the period of 3.7 d, in phase with the 3.56 d radial-velocity variations of Setiawan et al. (2008), appears to be one such 'tone'. It does not seem to be related to a possible planet orbiting TW Hya because it disappeared within one year. However – contrary to the clear period changes observed in 1.5 month of the MOST observations in 2008 – it was relatively stable through the three months of the 2007 radial-velocity observations.

The wide range of variability frequencies suggests a multitude of mechanisms. While we suspect that the main mechanism in the range of time-scales accessible to MOST is accretion within the innermost disc at distances of 2–15 $R_\odot$ from the star, it is hard to imagine that accretion would produce photometric variability on time-scales of years at the implied radii of several astronomical units. Thus, in the symphony orchestra analogy, more instruments (mechanisms) must be contributing to create the extended, well-defined flicker-noise variability spectrum of TW Hya.

ACKNOWLEDGMENTS

The Natural Sciences and Engineering Research Council of Canada supports the research of DBG, JMM, AFJM and SMR. Additional support for AFJM comes from FQRNT (Québec). RK is supported by the Canadian Space Agency and WWW is supported by the Austrian Space Agency and the Austrian Science Fund. GP acknowledges the research grant N20300731/1328 from Polish Ministry of Science.

Special thanks are extended to Ray Jayawardhana, Marten van Kerkwijk and Alexis Brandeker for very useful comments and to John Percy for an excellent review.

This research has made use of the SIMBAD data base, operated at CDS, Strasbourg, France and NASA's Astrophysics Data System (ADS) Bibliographic Services.

REFERENCES

Alencar S. H. P., Batalha C., 2002, ApJ, 571, 378
Daubechies I., 1992, Ten Lectures on Wavelets. Society for Industrial and Applied Mathematics, Philadelphia, PA
de la Reza R., Torres C. A. O., Quast G., Castilho B. V., Vieira G. L., 1989, ApJ, 343, L61
Grankin K. N., Melnikov S. Y., Bouvier J., Herbst W., Shevchenko V. S., 2007, A&A, 461, 183
Grassberger P., Procaccia I., 1983, Phys. Rev. Lett., 50, 346
Herbig G. H., 1978, in Mirzoyan L. V., ed., Problems of Physics and Evolution of the Universe. Publ. Armenian Acad. of Sci., Yerevan, p. 171
Herbst W., Herbst D. K., Grossman E. J., 1994, AJ, 108, 1906
Huélamo N. et al., 2008, A&A, in press (arXiv:0808.2386)
Jayawardhana R., Coffey J., Scholz A., Brandeker A., van Kerkwijk M. H., 2006, ApJ, 648, 1206
Koen C., Eyer L., 2002, MNRAS, 331, 45
Krist J. E., Stapelfeldt K. R., Ménard F., Padgett D. L., Burrows C. J., 2000, ApJ, 538, 793
Lawson W. A., Crasue L. A., 2005, MNRAS, 357, 139
Lehto H. J., Czerny B., McHardy I. M., 1993, MNRAS, 261, 125
Matthews J. M., Kusching R., Guenther D. B., Walker G. A. H., Moffat A. F. J., Rucinski S. M., Sasselov D., Weiss W. W., 2004, Nat, 430, 51
Paczyński B., Szczygieł D., Pilecki B., Pojmański G., 2006, MNRAS, 368, 1311
Percy J. R., Gryc W. K., Wong J. C.-Y., 2006, PASP, 118, 1390
Press W. H., 1978, Comments Astrophys., 7, 103
Pojmański G., 1997, Acta Astr., 47, 467
Pojmański G., 2002, Acta Astr., 52, 397
Pojmański G., 2004, Astron. Nachr., 325, 553
Pojmański G., Maciejewski G., 2005, AcA, 55, 97
Qi C. et al., 2004, ApJ, 616, L11
Rucinski S. M., 1988, Inf. Bull. Var. Stars, 3146
Rucinski S. M., Krautter J., 1983, A&A, 121, 217
Setiawan J., Henning Th., Launhardt R., Müller A., Weise P., Kürster M., 2008, Nat, 451, 38
Song I., Zuckerman B., Bessell M. S., 2003, ApJ, 599, 342
Torrence C., Compo G. P., 1998, Bull. Am. Meteorol. Soc., 79, 61
Torres G., Guenther E. W., Marschall L. A., Neuhäuser R., Latham D. W., Stefanik R. P., 2003, AJ, 125, 825
van Leeuwen F., 2007, Hipparcos, the New Reduction of the Raw Data. Springer, Berlin
Voges W., Atmanspacher H., Scheingraber H., 1987, ApJ, 320, 794
Walker G. et al., 2003, PASP, 115, 1023
Webb R. A., Zuckerman B., Platais I., Patience J., White R. J., Schwartz M. J., McCarthy C., 1999, ApJ, 512, L63
Wichmann R., Bastian U., Krautter J., Jankovics I., Rucinski S. M., 1998, MNRAS, 301, L39
Zuckerman B., Webb R. A., Schwartz M., Becklin E. E., 2001, ApJ, 549, L233

SUPPORTING INFORMATION

Additional Supporting Information may be found in the online version of this article.

Table 1. TW Hya: MOST 2007 and 2008 observations; single data points per each satellite orbit.
Table 2. ASAS photometric data for TW Hya, 2001–2008.

Please note: Wiley-Blackwell are not responsible for the content or functionality of any supporting materials supplied by the authors. Any queries (other than missing material) should be directed to the corresponding author for the article.

This paper has been typeset from a TEX/LATEX file prepared by the author.